

Climate Change and Extreme Events

Climent Ramis , Maria F. Cardell, Arnau Amengual , Romualdo Romero , Victor Homar , Sergio Alonso, and Agusti Jansa

Universitat de les Illes Balears, Palma, Spain

1 Introduction

It is nowadays fully accepted that a rapid human-induced climate change is affecting our planet. More than 97% of the scientific papers dealing with the issue agree on this fact [1], which is also endorsed by the main environmental scientific institutions of all countries. Climate change is undoubtedly one of the main challenges that twenty-first century societies will need to cope with, even in the most optimistic scenario where proper technologies may be developed to mitigate some of its worse potential effects. This challenge owes to the important influences of climate on health, environment, migrations, and economy, among other sectors. There are many physical indicators that can be considered when analyzing the problem of climate change, however, in this article, only temperature and precipitation will be discussed.

2 Observations

One of the clearest signatures of climate change is the global increase in temperature that the Earth is undergoing. This change is forced, with a very high probability (greater than 95%, [1]), by the increase in the atmospheric concentration of carbon dioxide and other greenhouse gases (methane, nitrogen oxides, and water vapor) as a result of fossil fuels consumption by human activities since the late nineteenth century and especially during the second half of the twentieth century. The concentration of carbon dioxide, measured at the observatory of Mauna Loa in Hawaii, has increased from a value of 315 parts per million in volume (ppmv) (Table 1) in 1958 to 410 ppmv in April 2018. The atmosphere has experienced important changes in the global concentration of CO₂ during its long history owing to natural factors, but such a rapid increase as the present

one seems unlikely in the proxy-derived reconstructions of CO₂ abundances over many millennia (Figure 1).

Regarding the warming of the atmosphere near the surface, Figure 2 shows the anomaly (with respect to the 1951–1980 average value) of the global mean temperature from the late nineteenth century until 2017. It is noteworthy that among the 17 years with highest temperatures, 16 belong to the twenty-first century, and also that 2016 has been the warmest year within the observed series (0.94 °C warmer than the twentieth century average, [4]). The mean temperature of the Earth has increased 1.1 °C since the late nineteenth century, but the increase attains 0.17 °C per decade since 1970. In the last years, the global mean temperature continues to rise even at a higher rate.

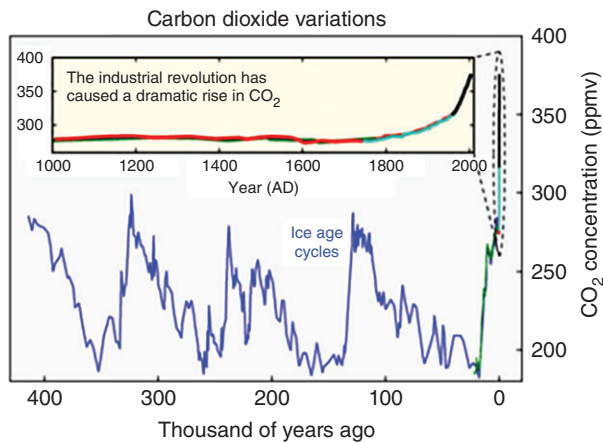
The temperature increase has not been uniform across the Earth (Figure 3). Warming signal dominates in almost all regions of the Earth, highlighting some areas of South America, and in the Northern Hemisphere such as North America, North Africa, and especially Eurasia. Interestingly, slight cooling is observed over a limited domain of the North Atlantic, south of Greenland.

Of crucial interest are all observed variations in global and regional rainfall due to the potential impacts on water availability for human consumption, agriculture, hydroelectric energy production, etc. It is remarkable that the increase of precipitation in the middle latitudes of both hemispheres (Figure 4) attributed to the greater capacity of a warmer atmosphere to hold water vapor and to the increased cyclonic activity in these latitudes. It is also noteworthy that the decreasing trend registered in the Mediterranean countries, in East Asia, and in the equatorial Africa. All these precipitation changes are particularly intense during the second half of the twentieth century.

There are many other evidences of the profound climate change that is taking place. Some well-marked

Table 1 Acronyms and terms included in this article.

ppmv	Parts per million in volume
NASA	National Aeronautics and Space Administration
MODIS	Moderate Resolution Imaging Spectrometer. Transported by Aqua and Terra satellites
EM-DAT	International Disaster Data-base. University of Louvain, Belgium
AOGCM	Atmospheric and oceanic global circulation model
IPCC	Intergovernmental panel on climate change
AR5	Fifth Assessment Report of IPCC
RCP	Representative Concentration Pathways. Emission scenarios considered in AR5 of IPCC
CMIP5	Coupled Model Intercomparison Project Phase 5
WMO	World Meteorological Organization
ITCZ	Intertropical convergence zone
CMIP3	Coupled Model Intercomparison Project Phase 3
SRES	Special Report on Emissions Scenarios. Emission scenarios considered in AR4 of IPCC
AR4	Fourth Assessment Report of IPCC
CDD	Consecutive dry days
RCM	Regional climate model
CORDEX	Coordinated Regional Climate Downscaling Experiment of the WCRP
WCRP	WMO World Climate Research Program
E-OBS	European Climate Assessment & Dataset project data-base
NOAA	National Oceanic and Atmospheric Administration

**Figure 1** Temporal evolution of CO₂ concentration in the Earth atmosphere. Source: [2].

trends (fully coherent with a warmer world) are variations in rainfall regimes, warming of the oceans, reduction of the ice cover in the Arctic, retreat of mountain glaciers, reduction of snow cover, increase of the mean sea level, and acidification of the oceans (Figure 5). The increases in the occurrence of extreme weather events (including heat and cold waves, torrential rains, flash floods, droughts, extraordinary tropical cyclones, intense midlatitude cyclones, and associated winds) are also especially relevant.

Most studies related to measures directed to the mitigation and/or adaptation to climate change have focused on the impacts driven by the changes in the mean climatic regimes [1]. However, a significant proportion of the climate change footprints, at least in terms of economic cost and loss of human lives, come associated with weather and climate extreme events (e.g. droughts, heat and cold waves, excessive precipitation, severe storms, cyclonic windstorms, etc.). A single storm of extraordinary intensity can lead to a quantitative damage equivalent to that produced by dozens of ordinary storms, or a severe drought lasting many months can exert much greater impacts than a long-term decrease in precipitation.

A meteorological or climatic extreme event by nature is a rare phenomenon; its adequate analysis thus requires very long data series in order to gain statistical significance of the results. There are different approaches for detecting extreme occurrences within a series. A certain threshold value can be defined and its exceedance would define an extreme (e.g. in relation to heat waves, the events for which the 30 °C temperature has been exceeded in a given place). Although this is a straightforward method, it poses interpretation challenges (the effects on the population are not the same when 30 °C are exceeded in July in Helsinki (Finland) or in Seville (Spain)). An alternative nonparametric approach to define thresholds, generally preferred, consists in isolating, for each location, the extreme occurrences based on

Figure 2 Variation of the mean temperature of the Earth. Anomalies respect the mean of the period 1951–1980. Source: [3].

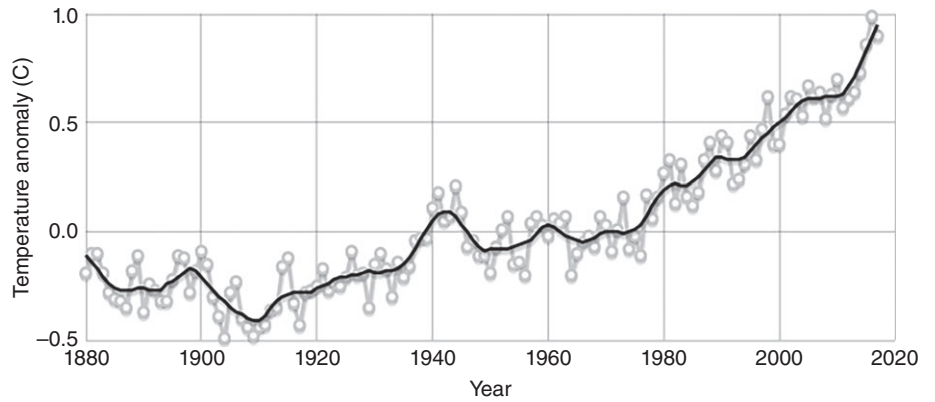


Figure 3 Spatial distribution of the observed change in surface temperature. Source: [1].

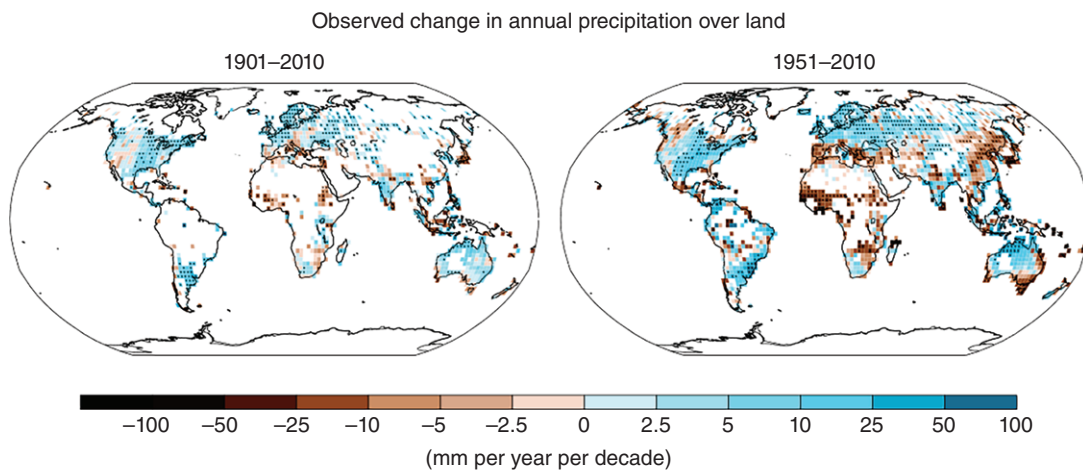
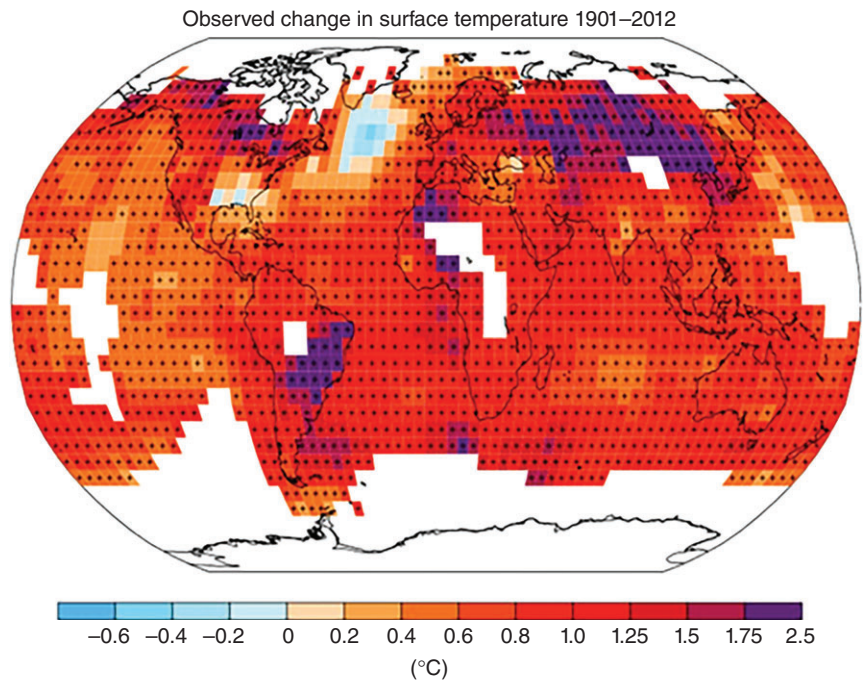


Figure 4 Observed changes in annual precipitation during the twentieth century and during the second half of the century. Source: [1].

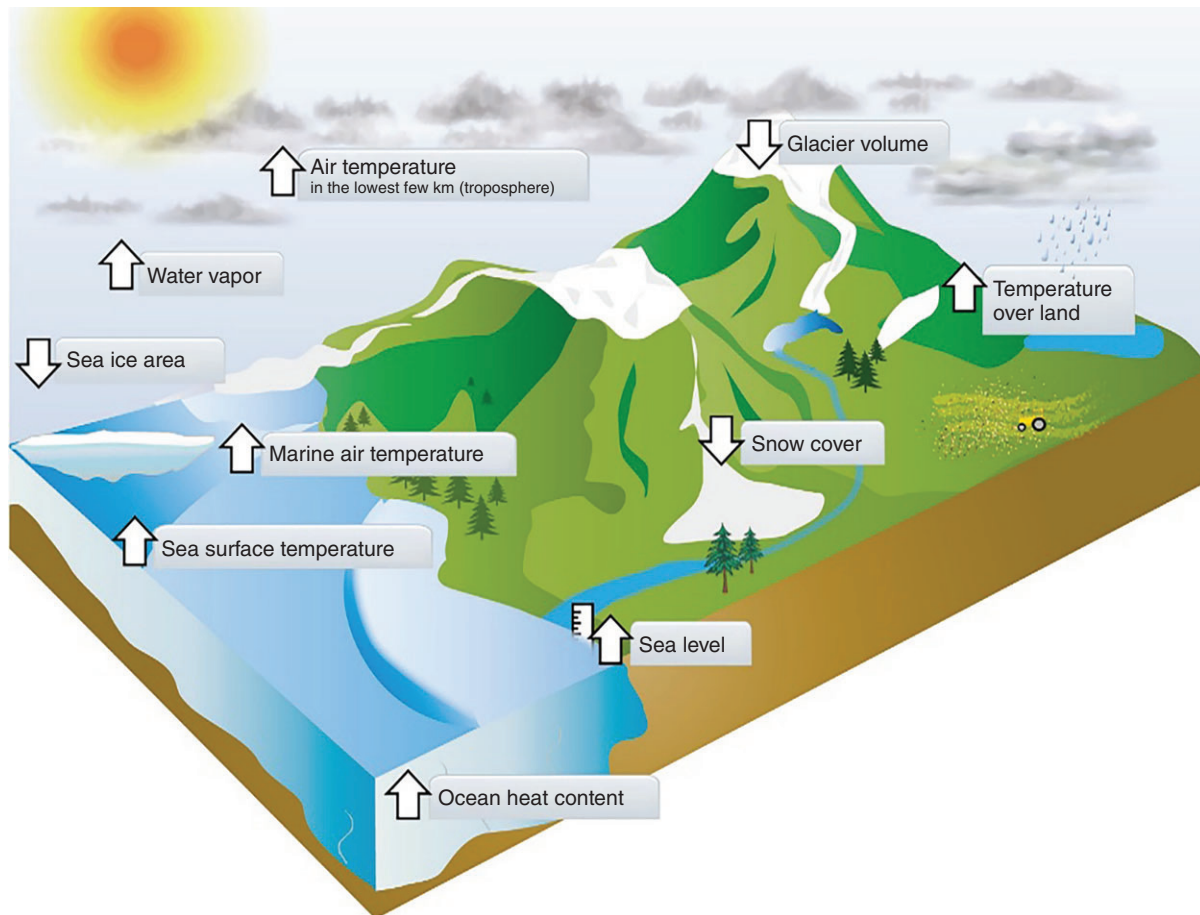


Figure 5 Diagram showing the clearest evidences of climate change. Arrows up (down) indicate increases (decreases). Source: [1].

the distribution of percentiles (e.g. the 95th percentile or the 5th percentile of the local temperature).

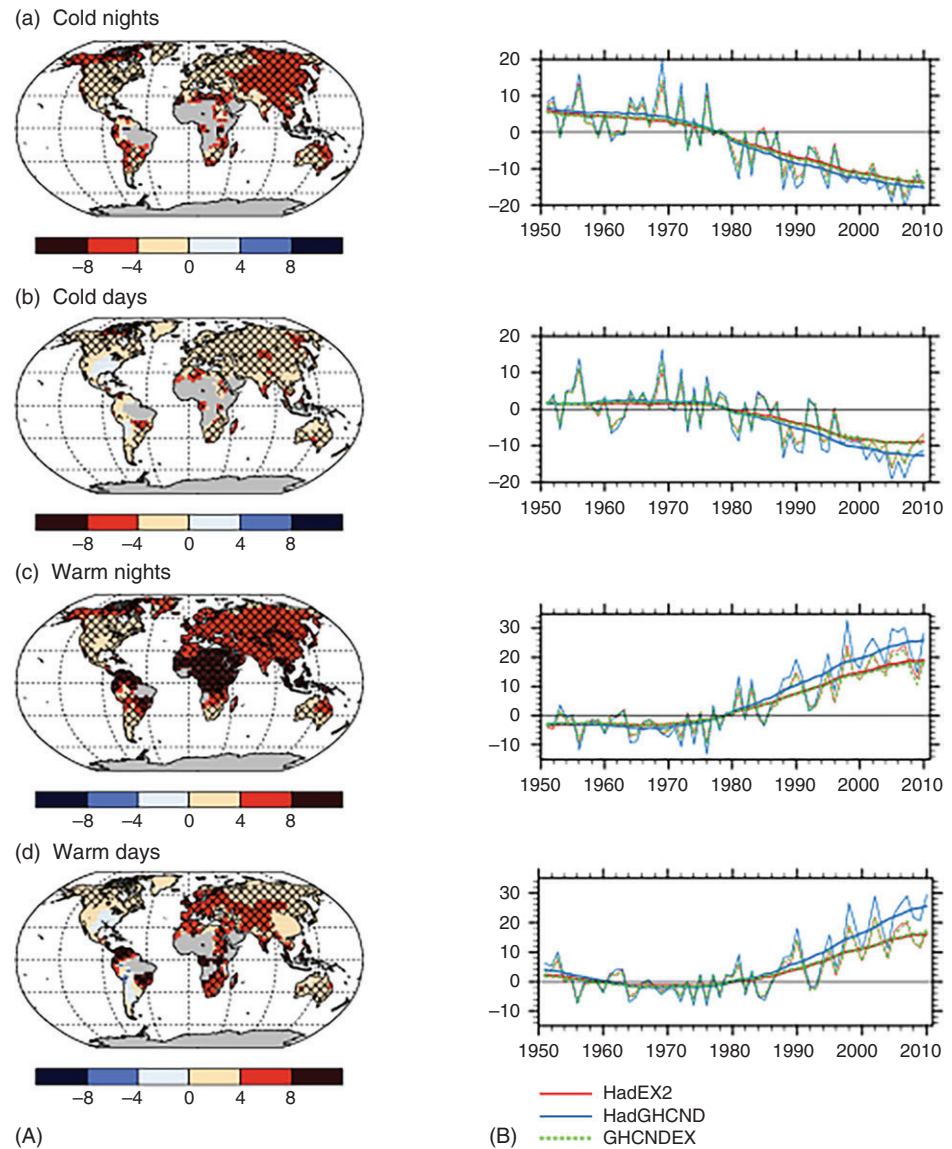
Globally, observations reveal that there has been a significant decrease in the occurrence of cold nights and cold days (Figure 6). Note that the decrease in cold nights is widespread over all continental lands, although more marked in Asia than in Europe and North America. With regard to the cold days, there is also a general decrease in the Eurasian continent, opposed to the increase observed in North America. Analogously and in line with the increase of the global mean temperature, there has also been a significant increase in the frequency of warm nights across the globe, with special incidence in Eurasian and Africa continents. Also, the frequency of warm days has increased significantly in Europe and parts of Asia and Africa (Figure 6).

Heat waves are one of the most outstanding anomalous behavior of temperatures due to the social implications they entail. Extreme and long-lasting heat waves (characterized by very high daytime and night temperatures in a continuous sequence of many days) have been

responsible for a marked increase in mortality, especially among elderly people. An extreme manifestation of this phenomenology and its hazardous effects was the 2003 European heat wave that hit the Western and Central parts of the continent during the summer (Figure 7). Surface temperature anomalies reach values as high as 10°C in France. It has been estimated that in Paris and Lyon, the heat wave augmented the mortality up to 75% during August 2003 [6]. In absolute estimated numbers, the mortality in Europe associated with this heat wave exceeded 70 000 [7].

During the summer of 2010, intense heat waves were registered in several zones of America and Asia. A particularly extreme heat wave affected Russia during the month of June. In Moscow, temperatures of 39°C were recorded and the highest values were reached in south-eastern Russia. Figure 8 shows the temperature anomalies during the period of greatest impact of the heat wave. This heat wave has been attributed to a very marked episode of La Niña. The European heat wave of 2010 is considered, in many aspects, more impacting than the aforementioned episode of 2003 (see [9]). This is

Figure 6 Spatial distribution of the changes in the number of annual cold and warm nights and cold and warm days during the second half of the twentieth century (A). Temporal evolution of the anomalies of the cold and warm nights and of the cold and warm days (B) obtained from three databases. Source: [5].



considered as one of the top 10 disasters by the EM-DAT INTERNATIONAL DISASTERS database [10].

Precipitation data exhibit significant changes in rainfall regimes during the second half of the twentieth century (Figure 9). Very intense rainfall, above the 95th percentile, has increased in eastern North America, central Europe, the Nordic countries, and in some regions of East Asia. Decreases are observed in western North America and southern Europe as well as in zones of East Asia. The same figure shows that the intensity of daily precipitation has increased in many regions of the Northern Hemisphere, but a decrease is noticeable in western North America, southern Europe, and some regions in Asia. Variation in the number of consecutive dry days (CDD) presents a spotty pattern being remarkable the increase of these dry periods in the Iberian

Peninsula. Finally, changes in an index that measures the extremity of the climate is included in the figure, although there are many regions with insufficient data as to permit a robust analysis of this issue.

3 Global Climate Projections

The atmospheric and oceanic global circulation models (AOGCM) are numerical climate simulation tools that are able to reproduce the current behavior of the climate system and therefore provide sufficient confidence for the simulation of the future climate. These sophisticated models account for the temporal evolution of the different components of the climate system (atmosphere, hydrosphere, cryosphere, lithosphere, and biosphere)

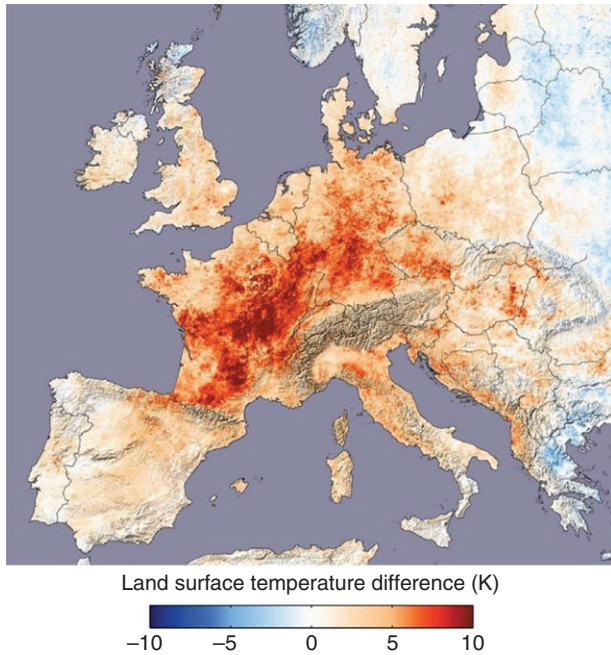


Figure 7 Land surface temperature anomalies during the 2003 summer heat wave in Europe. Source: Image by Reto Stöckli, Robert Simmon, and David Herring, NASA Earth Observatory, based on data from the MODIS land team.

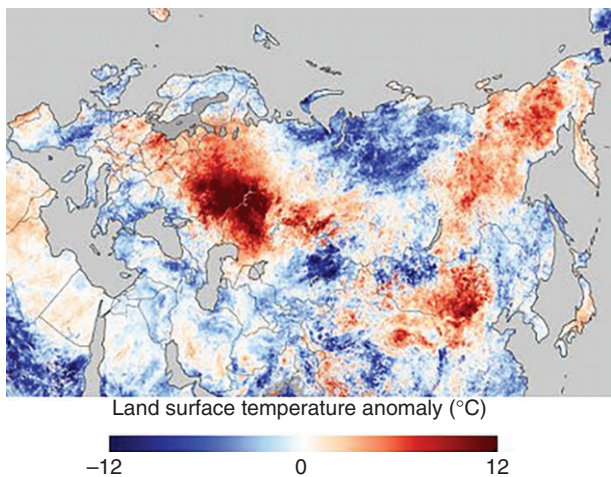


Figure 8 Land surface temperature anomalies during the 2010 summer heat wave in Russia. Source: [8].

and their complex interactions. The IPCC Fifth Assessment Report (AR5 [1]) presents, among others products, average results obtained from various climate models based on a set of scenarios for anthropogenic forcing. A new set of scenarios, the Representative Concentration Pathways (RCPs), was used for the most recent climate simulations of the twenty-first century carried out in the framework of the Coupled Model Intercomparison Project Phase 5 (CMIP5) of the WMO World Climate

Research Program (WCRP). In all RCPs (2.6, 4.5, 6.0, and 8.5), atmospheric CO_2 concentrations are higher in 2100 relative to present day as a result of a further increase in cumulative emissions of CO_2 to the atmosphere during the twenty-first century. They are identified by their approximate total radiative forcing in year 2100 relative to 1750: 2.6 Wm^{-2} for RCP2.6 (very low forcing), 4.5 Wm^{-2} for RCP4.5, 6.0 Wm^{-2} for RCP6.0 (stabilization scenarios), and 8.5 Wm^{-2} for RCP8.5 (very high forcing).

Figure 10 shows the projection for the twenty-first century of the global average temperature corresponding to two climatic scenarios, RCP2.6 and RCP8.5, with respect to the average temperature of 1985–2006. Even in the case of very low anthropogenic forcing, the CMIP5 models indicate a projected global mean surface temperature $1.0 \text{ }^\circ\text{C}$ higher than the current one on average, with a dispersion among the models of $\pm 0.75 \text{ }^\circ\text{C}$. For very high forcing (RCP8.5), the mean warming projected by 39 models is $4 \text{ }^\circ\text{C}$, with a dispersion exceeding $1 \text{ }^\circ\text{C}$.

Warming by the end of the twenty-first century is not uniform. Figure 11a shows the spatial distribution of the projected temperature changes under two extreme scenarios (low forcing and high forcing) with respect to the values observed in the period 1986–2005. It can be observed that under RCP2.6 the warming is rather general in all the areas of the Earth, but greater over lands than over the oceans and especially remarkable in the Arctic, with values in excess of $2 \text{ }^\circ\text{C}$. Antarctica also shows an increase of temperatures but less important than that projected over the polar zones of the Northern Hemisphere. For the RCP8.5 scenario, the temperature increase is also widespread, with values above $5 \text{ }^\circ\text{C}$ for a large part of the terrestrial zones of the Northern Hemisphere and a warming in excess of $9 \text{ }^\circ\text{C}$ for the Arctic polar zones. According to the projections, the polar zones of the Southern Hemisphere would not experience such extreme warming, with temperature increases in the range of $4\text{--}5 \text{ }^\circ\text{C}$.

With regard to precipitation, Figure 11b displays for the same scenarios the spatial distribution of the projected changes by the end of the twenty-first century with respect to the values observed at the end of the twentieth century. In both scenarios, an increase in precipitation is indicated in the intertropical convergence zone (ITCZ), especially over the Pacific Ocean. Also noteworthy is the increase in precipitation at high and midlatitudes in the Northern Hemisphere and some zones of the Southern Hemisphere. For the tropics, a decrease in precipitation is projected in both hemispheres. These changes are much more intense for the RCP8.5 scenario, in the order of 30% (in some areas even higher) for both increases and decreases. It is remarkable that the strong decrease in rainfall that is projected for the Mediterranean area. The

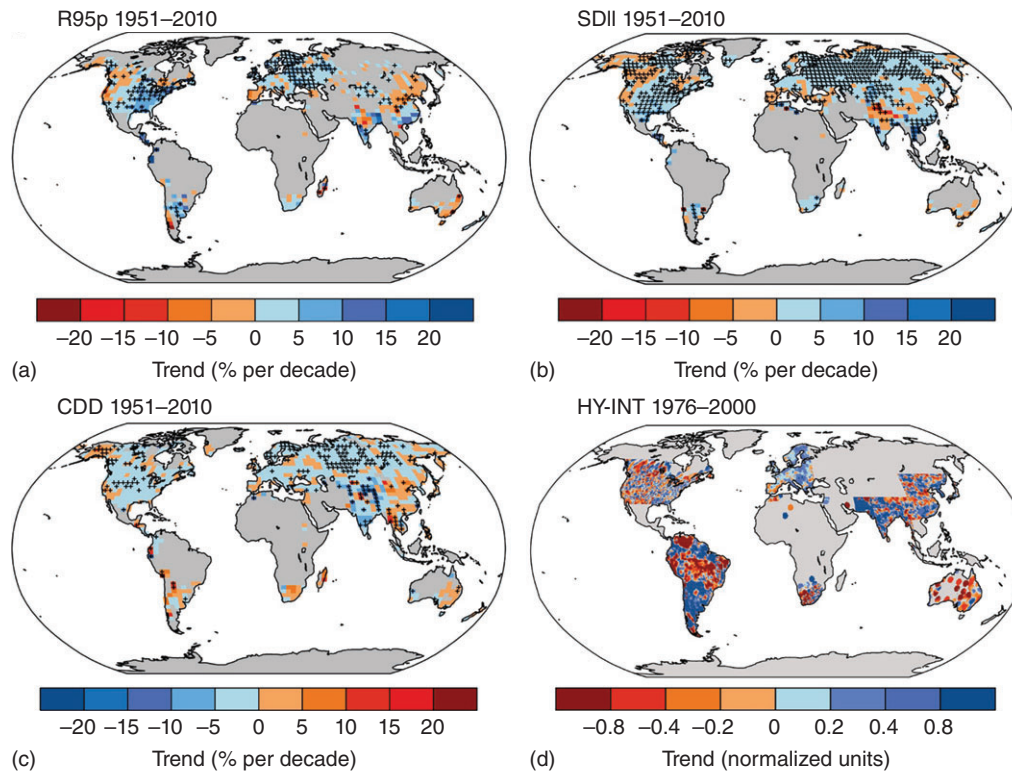
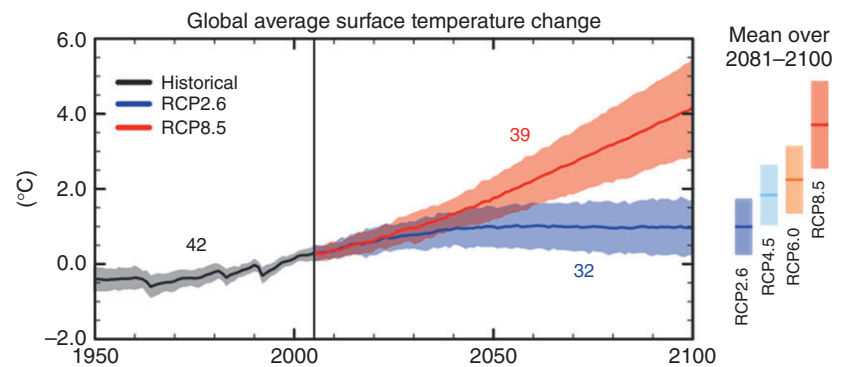


Figure 9 Trends in panels (a) intense precipitation ($R > 95\%$), (b) daily intensity (SDII), (c) consecutive dry days (CDD), and (d) HYDROCLIMATIC INTENSITY as an indicator of climate extremes. Source: [1].

Figure 10 Projection of the global average temperature of the Earth under the scenarios RCP2.6 and RCP8.5. The shown numbers correspond to the number of CMIP5 models used. The shaded bands indicate the spread shown by the models. On the right, the accumulated warming projected in the four RCP scenarios for 2081–2100 is shown, mean value and spread. Source: [1].



combination of increasing temperature and decreasing precipitation can lead to intense changes in the water balance of the region and strong impacts on the economy in countries that depend strongly on tourism [11].

The average tendencies obtained from the models are complemented with the corresponding inter-model spread which in part accounts for the climatic variability. Within this variability, it should be taken into account the presence of extreme values that are ultimately responsible for the strongest impacts of climate change on many aspects of life. Figure 12a shows the projection on a global scale of the percentage of days in which the current climate 90th percentile temperature is exceeded

according to different climatic scenarios. A clear increase of warm days can be observed for the three scenarios but especially in RCP8.5; this indicates an increase in the number of heat waves. Those observed in 2003 and 2010 in Europe would probably not be exceptional but frequent under this scenario. Analogously, Figure 12b shows the percentage of temperature events below the 10th percentile. The projected decrease of cold days is evident.

Figure 13 shows the spatial distribution of the expected future variation of warm nights (the minimum temperature exceeds the 90th percentile), cold nights (the temperature is below the 10th percentile), and

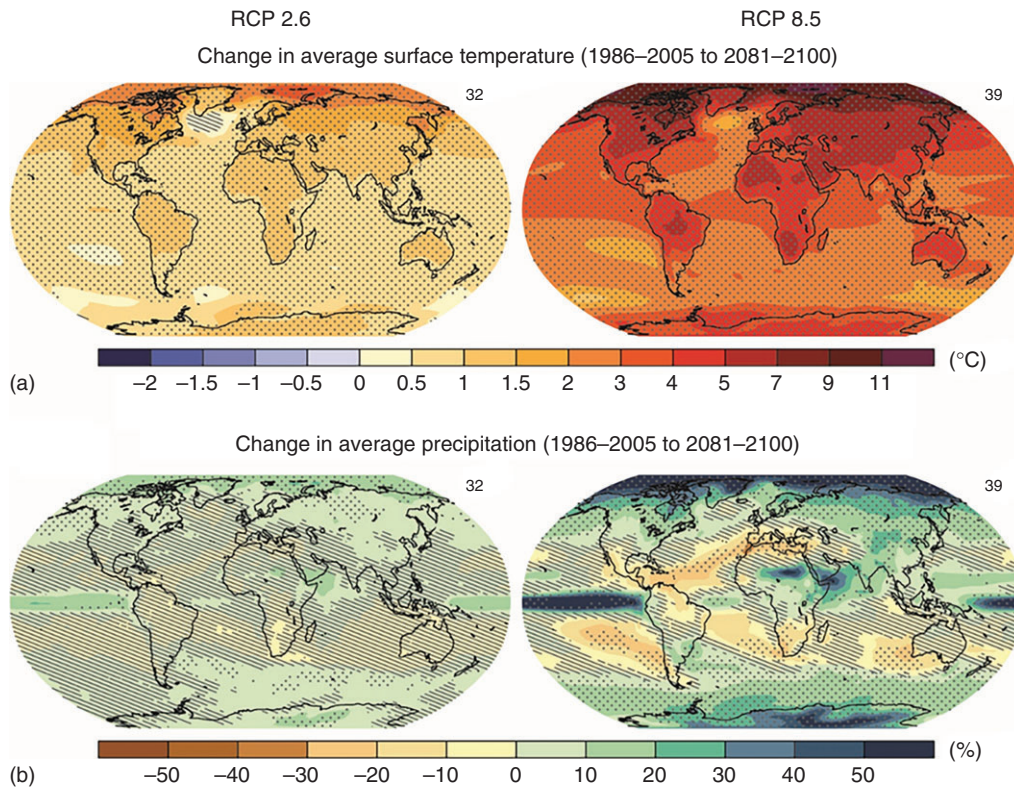


Figure 11 (a) Projections of the spatial distribution of the temperature change for the period 2081–2100 with respect to 1986–2005 for the scenarios RCP2.6 and RCP8.5 and (b) projections of the spatial distribution of the change in rainfall between same periods and for the same scenarios. The numbers in the upper right corner of the panels indicate the number of models used. Source: [1].

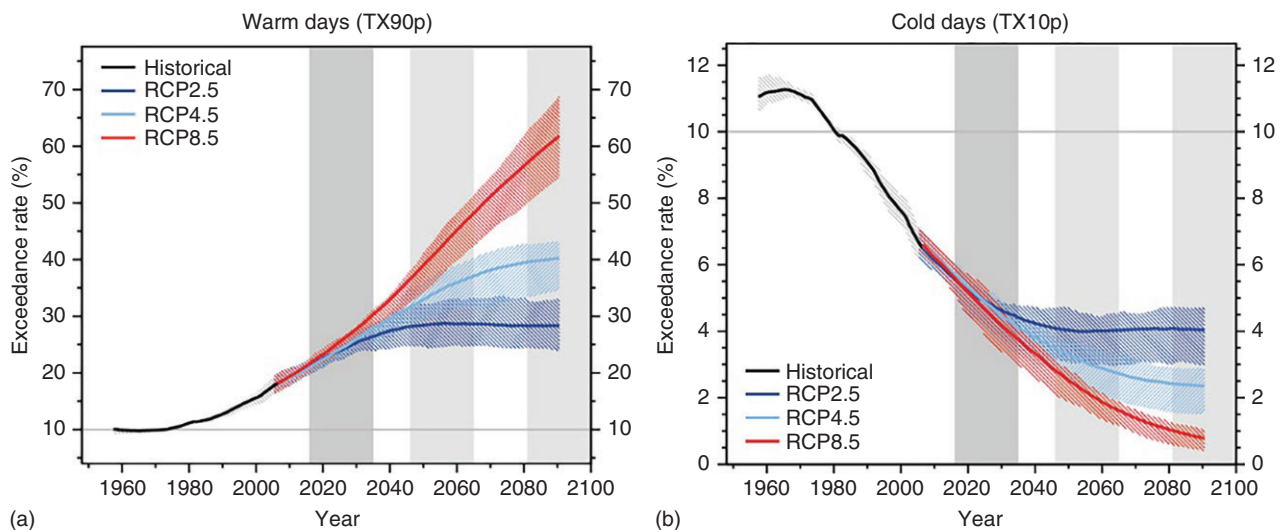


Figure 12 Temporal evolution of the exceedance rate of warm days (temperatures above the 90th percentile) and cold days (temperatures below the 10th percentile) during the twenty-first century for three RCP climatic scenarios. Source: [1].

the percentage of days with minimum temperatures above 20 °C (tropical nights) for the period 2080–2100 compared to the 1960–1999 reference. This product was obtained from 14 AOGCM contributing to the CMIP3 project (based on simulations under emission

scenario SRES A2 considered in the IPCC AR4 [13]). The annual change and the changes for winter (December, January, and February) and summer (June, July, and August) are considered. An increase of warm nights is expected in practically all areas of the Earth, especially

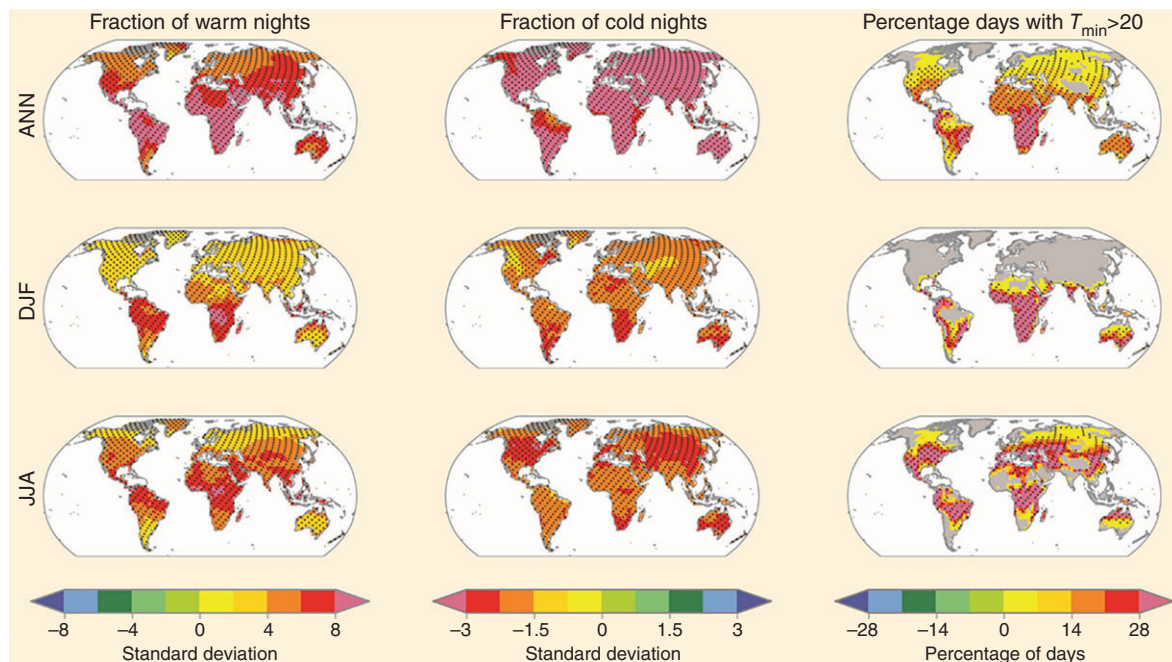


Figure 13 Spatial distribution of the expected change in warm and cold nights for the period 2081–2100 compared to 1960–1999. In the third column, the spatial distribution of the percentage change of days with minimum temperature above 20 °C. Source: [12].

at midlatitudes during the corresponding summer of the hemisphere. Consequently, a decrease in the frequency of cold nights is expected at all latitudes, most remarkable over the mid and high latitudes of both hemispheres. The percentage of tropical nights also shows an increase, especially in JJA in the Northern Hemisphere.

Analogous spatial distributions of the projected variation of warm days (maximum temperature above the 90th percentile), cold days (minimum temperature below the 10th percentile), and the percentage of days with maximum temperatures above 30 °C are shown in Figure 14 for the full year and for the seasons of winter (December, January and February, DJF) and summer (June, July and August, JJA). A remarkable increase in warm days in all latitudes and a decrease in cold days are projected, especially when considering the annual results. A noticeable increase in the percentage of days with temperatures above 30 °C is also projected.

An increase in extreme precipitations is compatible with the increase in temperatures. The ability of the atmosphere to hold water vapor increases with temperature. Figure 15 shows the spatial distribution of the projected change (2081–2100 vs 1961–1990, annual scale, winter, and summer) in the percentage of days with precipitation above the 95% percentile. The maps indicate an increase in days with intense rainfall in most of the Northern Hemisphere at high latitudes, especially in winter. Increases are also projected in the Southern Hemisphere during the winter in the equatorial zones

of South America and Africa. We can also highlight the decrease in the days with heavy rain in the Mediterranean, a region where convective type rains abound. A decrease is also observed in Southeast Asia in winter and in South America and South Africa during JJA.

The projected increase in the number of heavy rain days is accompanied by significant changes in the occurrence of dry periods, thus indicating accentuated modifications in the future rainfall regimes in many areas. Figure 16 shows the spatial distribution of the change in the occurrence of CDD for the period 2081–2100 with respect to 1980–1999. By mid-twenty-first century, this index is expected to increase in wide areas, especially in the Mediterranean zone, but a decrease is projected in high latitudes of the Northern Hemisphere. By the end of the twenty-first century, the spatial pattern of CDD changes is very similar, but the amounts (both positive and negative) are now much more intense, that is there is an intensification in the change of rainfall regime frequencies. The Mediterranean area and the south of Europe stand out once again, exhibiting a sharp increase in the length of the dry periods.

4 Regional Climate Models

The spatial resolution of global models is sufficient to project the climate at large scales; however, it does

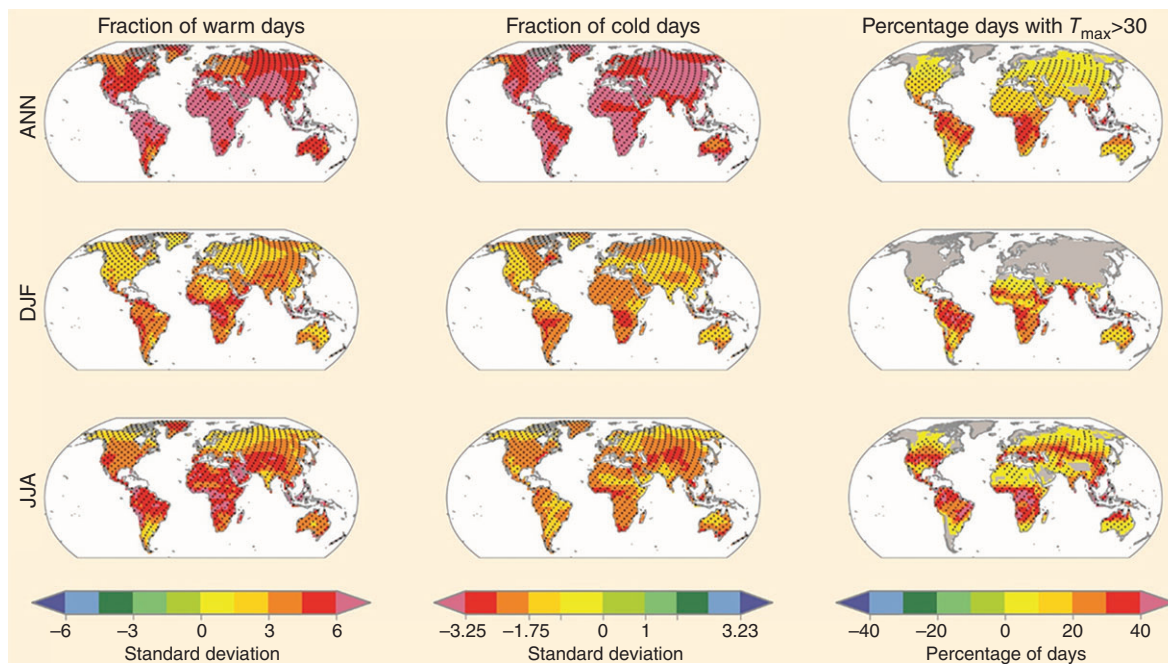


Figure 14 Spatial distribution of the expected change in warm and cold days for the period 2081–2100 compared to 1960–1999. In the third column, the spatial distribution of the percentage change of days with a maximum temperature of 30 °C is shown. Source: [12].

not allow resolving relevant processes related to local features, such as the orography. The study of extreme events also suffers from the lack of resolution in global models. It becomes necessary to transfer adequately the projections from global to regional and local scales by carrying out some downscaling process. A widely used method is to run climate models within a limited area at much higher spatial resolution than global models, nesting this regional simulation in some global model [14]. The method is known as dynamic downscaling. Even the results of these models are difficult to adapt locally due to imperfections in the description of physical phenomena and other processes.

The issue is aggravated when daily data and extreme values are analyzed, since incorrect statistical distributions simulated by a model for a given meteorological variable may lead to wrong conclusions. Although RCMs often improve the performance of AOGCMs at regional scales, the used spatial resolutions still remain inadequate to address uncertainties emerging from different sources and obtain information at local scales.

The results previously shown, corresponding to AOGCM, display that in many aspects Europe will undergo important changes in both temperature and precipitation. Also that the impacts will be different for northern Europe and southern Europe, a notion quite evident when comparing the projections for the northern countries with those obtained over the Mediterranean area. Similar conclusions have been

highlighted using RCM by Giorgi and Lionello [15] and Ramis and Amengual [16]. Especially interesting are the new projections for Europe obtained with the RCM of the EURO-CORDEX project, the European contribution to the CORDEX project [17].

To obtain projections at local scales, the results of the RCM must be subjected to some adjustments that are inferred by comparing model results for a certain reference period with the local observations for that same period. This adjustment process is known as statistical downscaling. The results shown below correspond to mean values of 14 RCM of the CORDEX project with a resolution of 12 km [18] modified locally by a quantile-quantile adjustment method developed by Amengual et al. [19] and improved by Cardell et al. [20]. Although the simulations of the CORDEX project have been carried out under different RCPs, the results shown below correspond to the RCP8.5 scenario. Observational information corresponding to the current climate comes from the E-OBS dataset [21].

Figure 17 shows the mean annual rainfall in Europe for the period 1981–2005, and the percentage change of the projected rainfall for 2071–2095. Regarding the projected trends, it must be highlighted the accentuated decrease in the Iberian Peninsula and northern Africa, Italy, Albania, Greece, southern Turkey, Lebanon, and Israel (the areas with Mediterranean climate). In some cases, this precipitation decrease is greater than 30%. This result represents a high impact since some of the

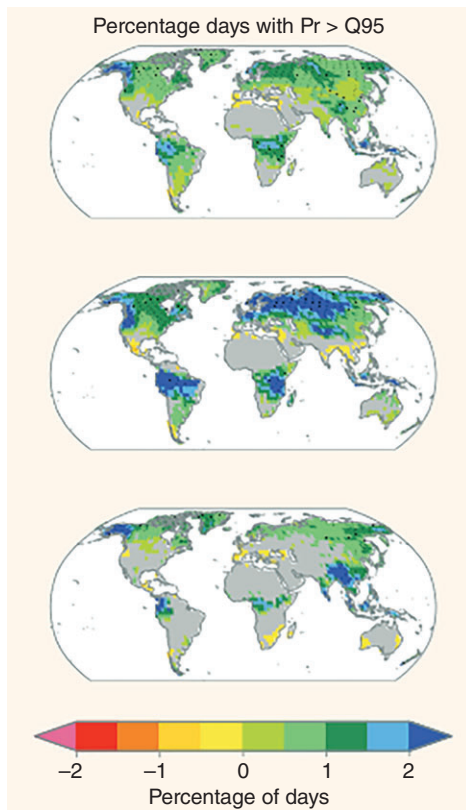


Figure 15 Projected annual and seasonal changes for 2081–2100 with respect to 1980–1999, based on 17 GCMs contributing to the CMIP3, of the percentage of days with precipitation above the 95% quantile, calculated from the 1961 to 1990 reference period. The changes are computed for the annual time scale (top) and two seasons (DJF, middle and JJA, bottom). Source: [12].

aforementioned zones already have scarce rainfall. A less intense decrease is also projected over France and countries with littoral in the Black Sea. On the other hand, a significant increase in precipitation is projected in the Scandinavian and Baltic countries and northern Russia.

Figure 18 shows the projected seasonal changes in precipitation at the end of the twenty-first century. There is a decrease in precipitation in southern Europe throughout the year, especially marked during the summer. In the south of the Iberian Peninsula, the decrease could be more than 40% during the summer and spring. In the Scandinavian countries, an increase in precipitation is projected throughout the year, especially in spring. In general terms, it is expected an increase in precipitation over central and northern Europe.

The number of precipitation days would suffer a significant decrease owing to climate change in most of the continent during all seasons, especially during summer and autumn. Figure 19 shows that the decreases can exceed 50% in spring and summer in many points of

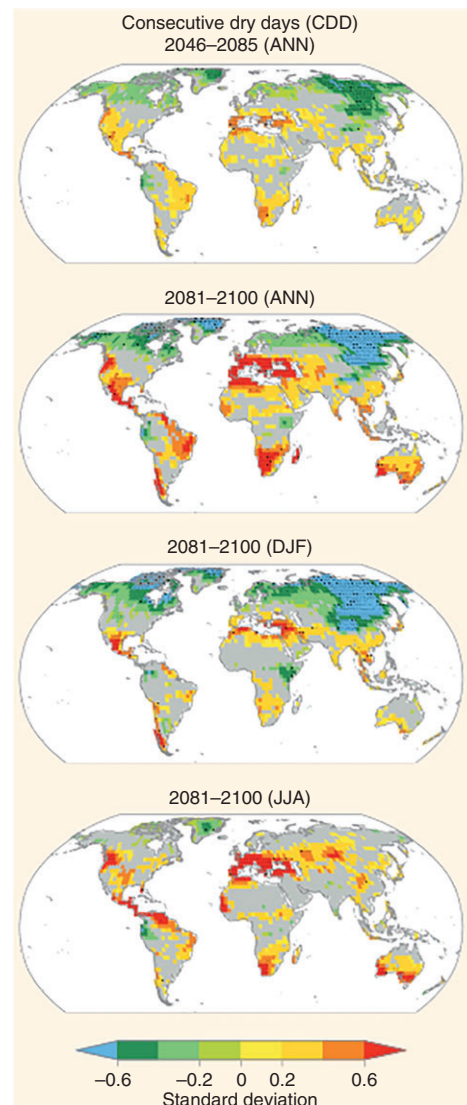


Figure 16 Spatial distribution of the projected changes in consecutive dry days (CDD, as a measure of drought) for the middle and end of the twenty-first century compared to 1980–1999. Mean values are presented for the periods 2046–2065 and 2081–2100, and for winter and summer for 2081–2100. Values obtained from 15 GCM corresponding to CMIP3. Source: [12].

the northernmost part of the Mediterranean countries. There is only an increase in precipitation days in the Scandinavian countries and Baltic Sea coastal regions during the spring. Bearing in mind that an increase in precipitation is expected over Central Europe for the autumn while a notable decrease in the number of precipitation days is expected, an increase in the intensity of rainfall in this area is projected, which would be compatible with an increase in precipitations of convective origin.

It is projected that the minimum temperatures in winter (Figure 20) suffer a marked increase in the Nordic

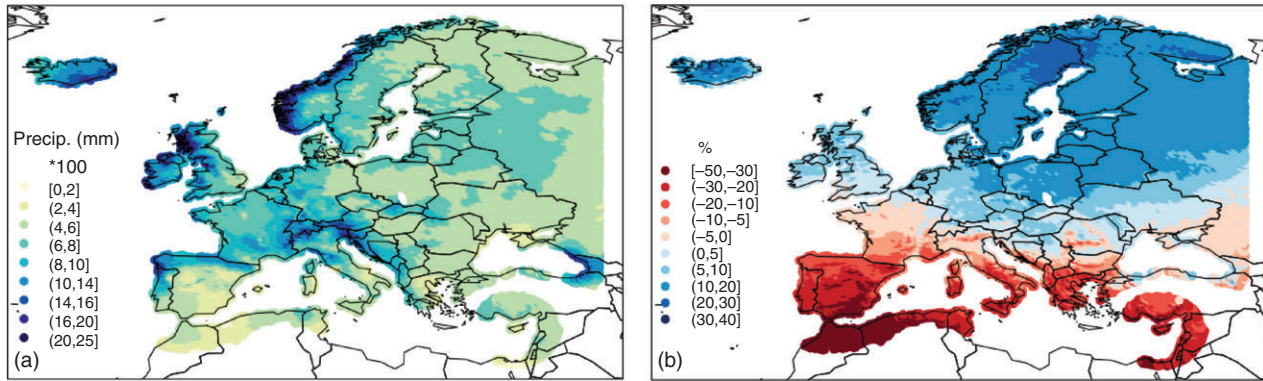


Figure 17 Mean annual rainfall in Europe for the period 1981–2005 (a) and the projected percentage change for the period 2071–2095 (b). Source: [20].

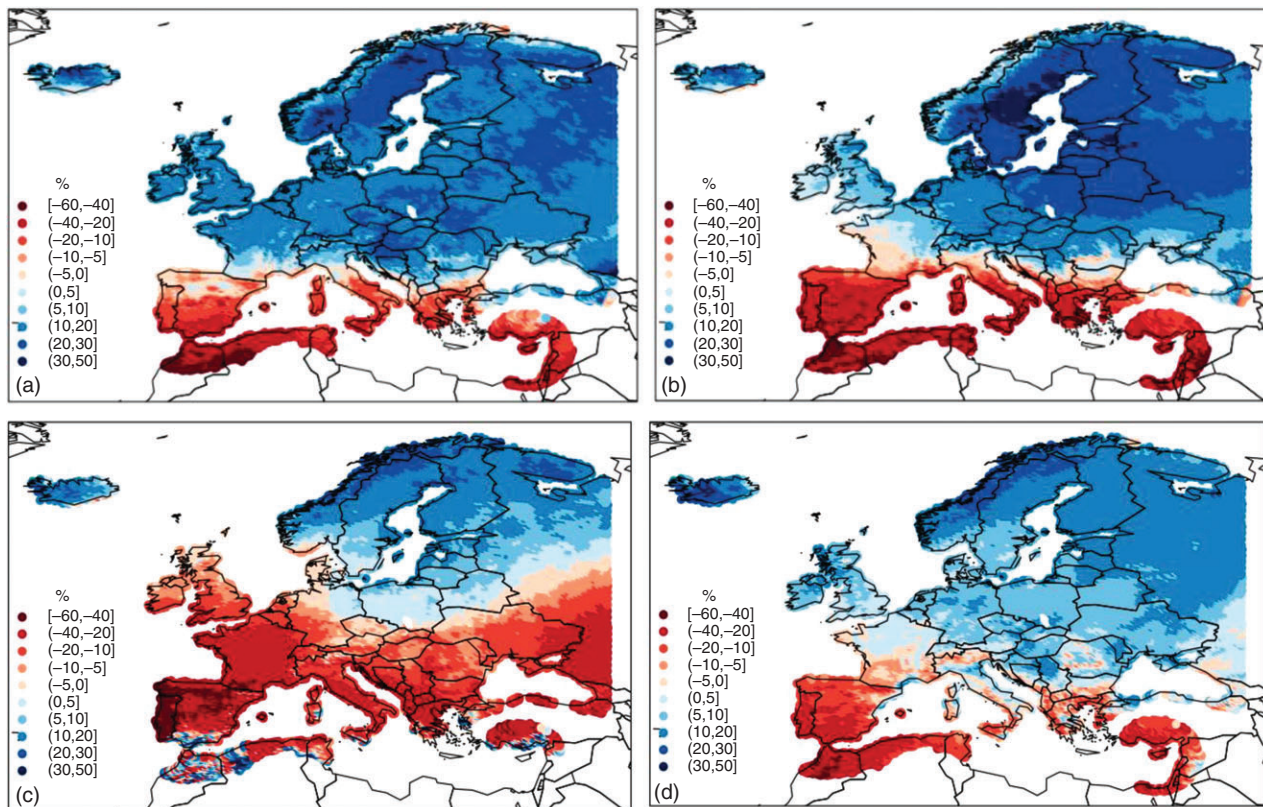


Figure 18 Percentage changes in precipitation for the period 2071–2095 for winter (a), spring (b), summer (c), and autumn (d). Source: [20].

countries that can exceed 7°C . In Central Europe, a less pronounced increase is also expected (around 4°C), although it is higher in the Alps and Pyrenees. In Western Europe (France, United Kingdom, Spain, and Italy), the projected increase is less marked. The spatial distribution of the expected changes in spring is similar to that of winter but the increases are less accentuated. However, in summer, it is expected that the greatest increase in minimum temperatures will occur in southern Europe (Iberian Peninsula, Italy, Greece, and Turkey,

i.e. countries with Mediterranean climate). In the highest latitudes of Europe, summer minimum temperatures are also expected to increase but in much lower magnitude than in winter. In Central Europe, the increases are also expected to be higher than in winter. During the autumn, a warming pattern is expected with a spatial distribution similar to that of spring but with somewhat higher values. In short, the minimum temperatures will increase throughout Europe but especially in the high-latitude regions and toward Central Europe during the winter,

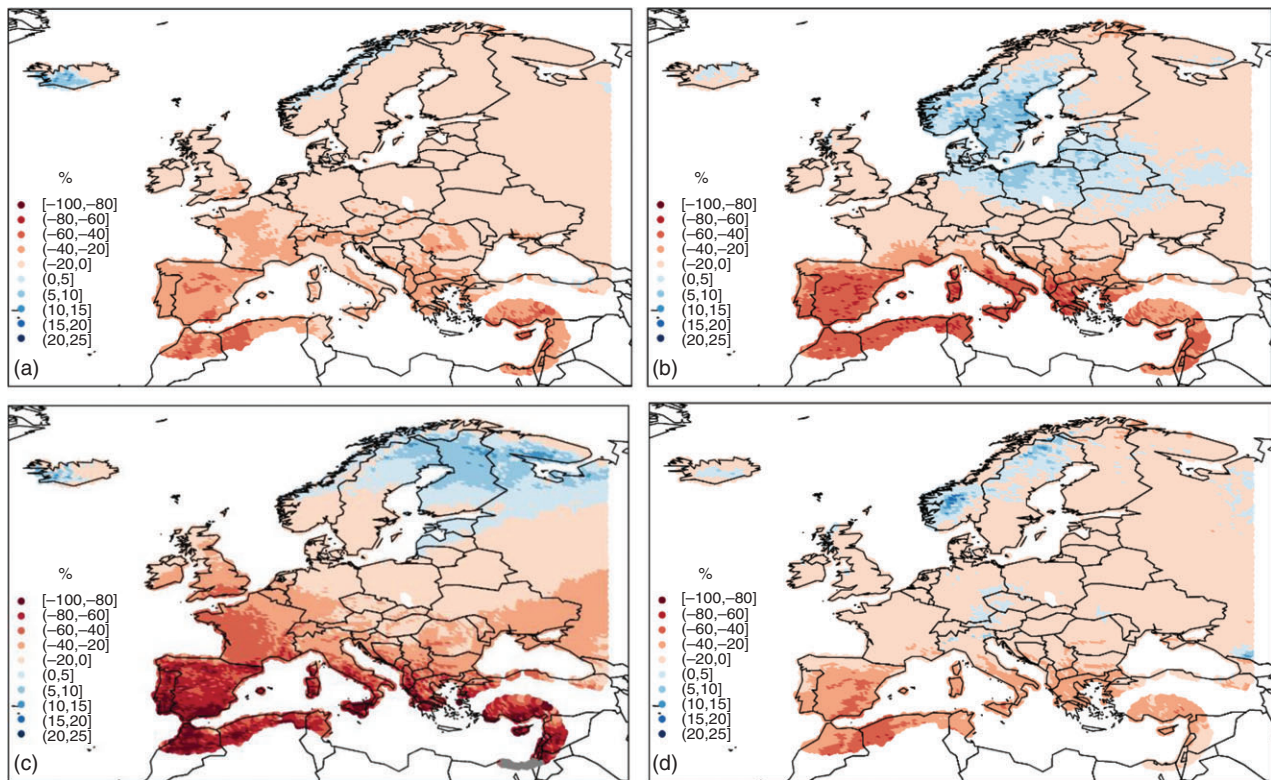


Figure 19 Spatial distribution of the projected change in the number of precipitation days for the period 2071–2095 in winter (a), spring (b), summer (c), and autumn (d). Source: [20].

spring, and autumn; however, the largest increases in summer are expected in the Mediterranean countries.

Regarding the spatial distribution of the projected changes in maximum temperature (Figure 21), it is expected an increase throughout Europe and throughout the year. Particularly in winter, the largest increases are expected in the north of the Scandinavian countries (up to 6 °C) extending to Central Europe and toward Turkey with somewhat lower values. For the western part of Europe (United Kingdom, France, and Iberian Peninsula), smaller increases are expected (about 2 °C and locally 3 °C). In spring, the same pattern is maintained, but larger increases in southern Europe and somewhat lower in Central Europe than in winter are expected. Again, the southern Europe countries exhibit the greatest increases in maximum temperatures with values that reach 5 °C. In autumn, the spatial distribution and the magnitude of the change are both similar to those of spring. These downscaling results highlight the large warming trend for minimum and maximum temperatures in the Mediterranean countries during the summer, which will lead to unbearably hot summers at the end of the century. The tendency toward more temperate climates in Nordic countries can also be highlighted, especially as a result of the increase in the minimum temperatures.

The analysis of severe events based on the locally adjusted RCM results of the CORDEX project provides outstanding information. Figure 22 shows the local values of the 95th percentiles of maximum temperatures, observed in the period 1981–2005 during the summer (that is only 5% of days reach warmer temperatures than the indicated thresholds). The figure also shows the percentage of days at the end of the twenty-first century presenting temperatures above the previous 95th percentile values. Regarding the spatial distribution of these extreme temperatures for the current climate, it should highlighted the high values found in the south of the Iberian Peninsula (above 35 °C), but also in southern Europe and central Europe, except for the Alps. The lowest values correspond to the Scandinavian regions and northern Russia. With regard to the future daily temperatures that at the end of the century will be in excess of the current 95th percentile, it can be seen that the percentage is low for the Scandinavian countries, the Baltic countries, northern Russia, and northern Central Europe. For Southern Europe (Iberian Peninsula, Greece, and Turkey), a very high percentage of days (even higher than 50%) will manifest these extreme temperatures in the future, which is indicative of a clear increase in the occurrence of heat waves. In the Middle East, this percentage could exceed the 70% level.

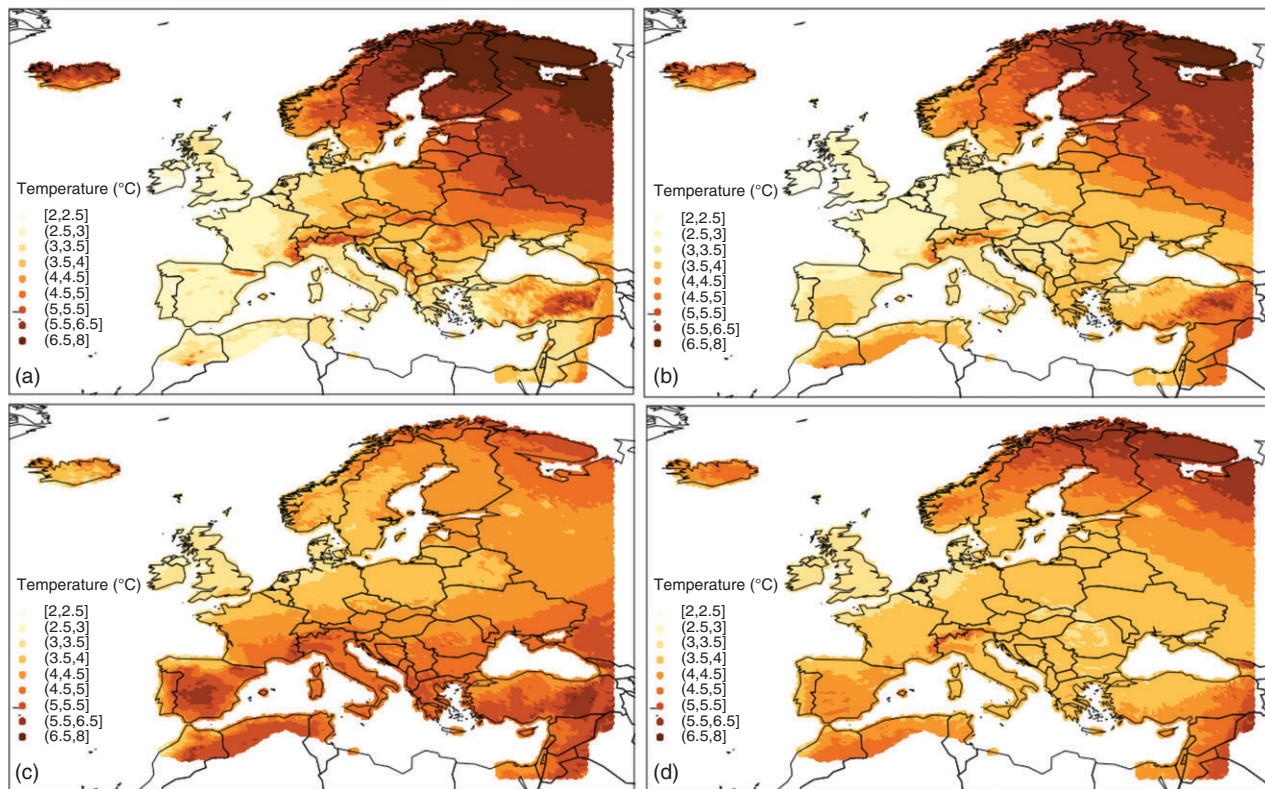


Figure 20 Spatial distribution of the projected change in mean minimum temperatures for the period 2071–2095 for winter (a), spring (b), summer (c), and autumn (d). Source: [20].

Regarding the problem of cold waves, Figure 23a shows the current spatial distribution of the 5th percentile (that is, only 5% of the observed minimum temperatures are below this limit) corresponding to the period 1981–2005 during winter. Most of Europe presents values below 0°C , only the southernmost areas have positive values. For the north of the Scandinavian countries and north of Russia, the values are lower than -30°C . In terms of the future percentage of minimum temperatures below the current 5th percentile (Figure 23b), very low values are expected for all of Europe, in any case, higher than 2%. This is an indication of fewer cold nights, but despite the warming, cold waves will not disappear completely in any European territory, including the south of the continent.

Recall from Figure 17 the projected changes in annual precipitation. The south of Europe will face a noticeable decrease in precipitation amounts, whereas in the northern countries an increase. The indicated decrease could imply an increase in the length of dry periods that could lead to significant droughts. Figure 24 shows the local 95th percentile of the length, in days, of dry spells in Europe. Central Europe, the Scandinavian and Baltic countries, and northern Russia exhibit values lower than 10 days, while the Mediterranean countries reach,

in some cases, up to 50 days. Figure 24 also presents the expected change in the number of episodes at the end of the twenty-first century (2071–2095) that will exceed in length the current 95th percentile thresholds. For northern and central Europe, a decrease in the occurrence of long dry episodes is expected (compatible with the increase in the number of precipitation days). For southern Europe, a slight increase in the number of persistent dry episodes is expected, which will also last longer than the current dry spells.

5 Possible Lines for Future Research in Climate Change

Climate science has progressed very significantly during the last decades. However, open questions still remain and advancing the knowledge of key processes controlling the climate system is of primary importance in order to address basic intellectual problems but also to confront the challenging impacts on society. Near future research will focus on better understanding climate processes, and especially those linked to cloud and aerosol dynamics, the couplings among the climate subsystems (atmosphere, hydrosphere, lithosphere, cryosphere, and

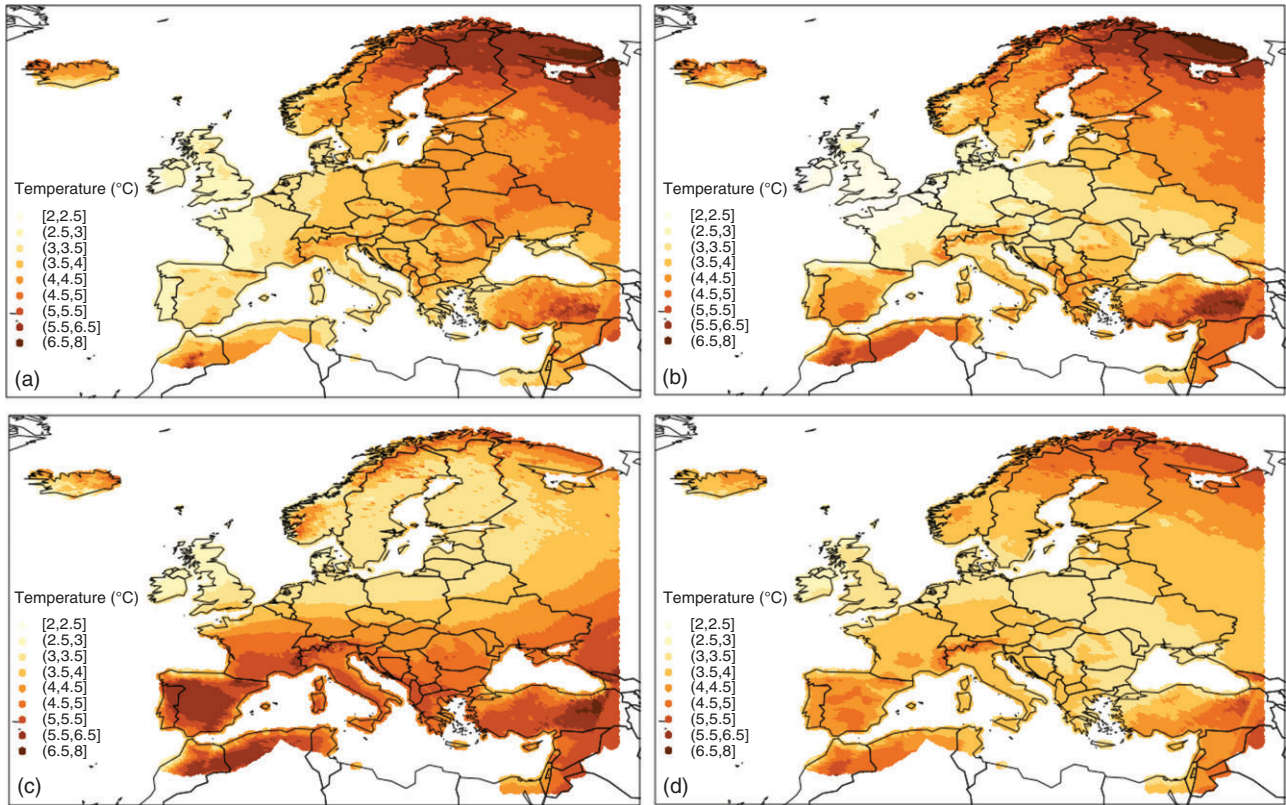


Figure 21 Spatial distribution of the projected change in mean maximum temperatures for the period 2071–2095 for winter (a), spring (b), summer (c), and autumn (d). Source: [20].

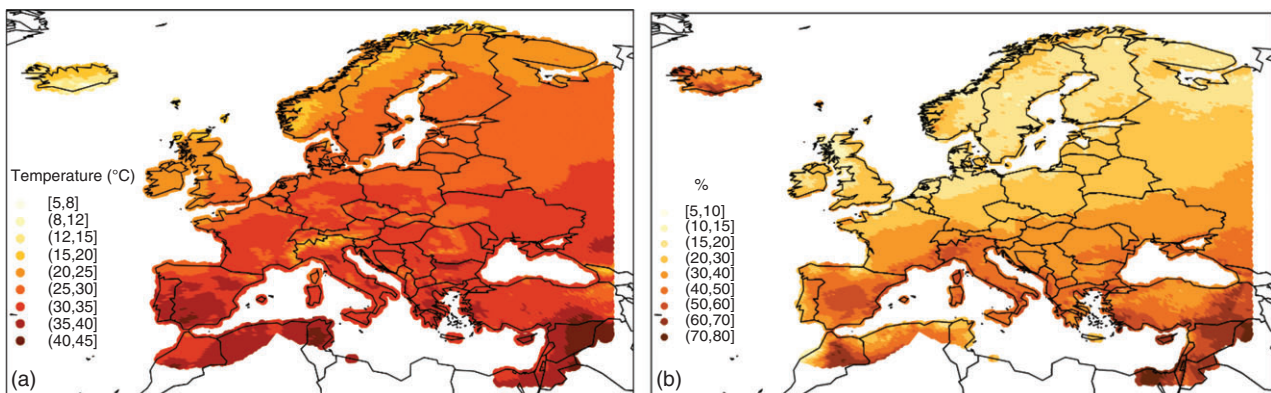


Figure 22 Maximum temperature 95th percentiles observed during the period 1981–2005 in summer (a) and the percentage of days that at the end of the twenty-first century will be warmer than the previous current climate percentiles (b). Source: [22].

biosphere). These improvements will allow to ameliorate current climate modeling systems beyond the natural spatial resolution increase, which will, in turn, allow to advance in the understanding of climate extremes. Indeed, understanding, modeling, and predicting climate extremes have been selected as one of the WCRP Grand Challenges. An additional field of active research in the coming years is the understanding and prediction of climate tipping points, which pose a difficult scientific

challenge and are expected to imply large socioeconomic impacts. A significant example is oceanic overturning circulations and their impacts on global energy fluxes and balances.

Regarding prediction tools, AOCGM models are a decisive instrument in the study of climate change. They have demonstrated their capacity to simulate the projections for the first decades of the twenty-first century which are really good. In recent years, the larger the

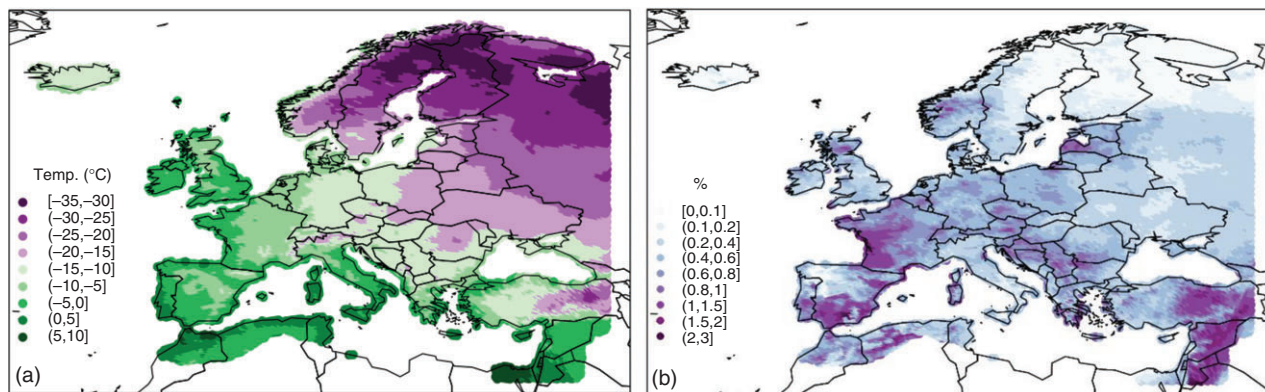


Figure 23 Minimum temperature 5th percentiles of observed during the period 1981–2005 in winter (a) and the percentage of days that at the end of the twenty-first century will be colder than the previous current climate percentiles (b). Source: [22].

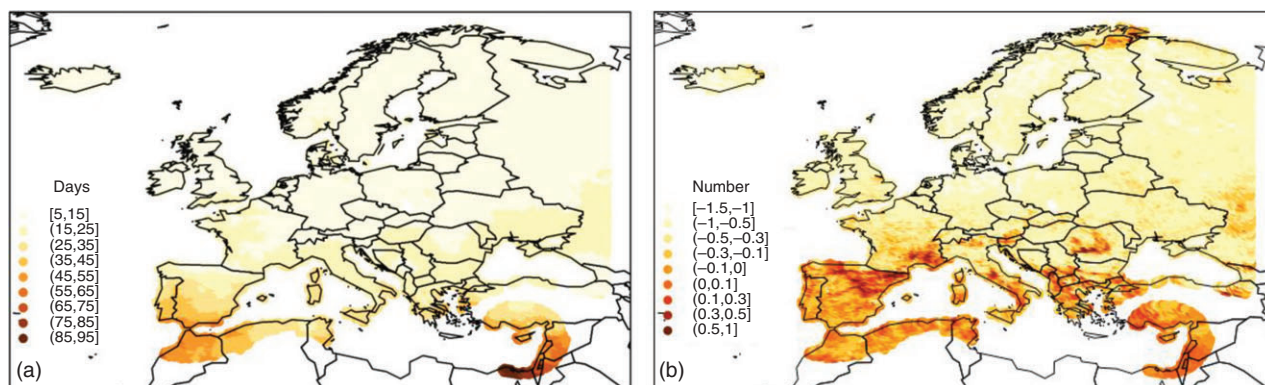


Figure 24 95th percentile values of the lengths of dry periods in the present climate 1981–2005 (a). Expected change in the number of episodes at the end of the twenty-first century (number of episodes in the future – number of observed episodes) that will last longer than the previous 95th percentile (b). Source: [22].

available computational resources, the more complex and realistic these models have become. The future increase in computing capacity will also be decisive in continue improving numerical climate projections. However, more precise and even new interactions between the subsystems that conform the climate system must be incorporated. The interactions between these systems are not completely known (e.g. influence of cryosphere on the ocean deep circulation). Some of these synergisms are also highly nonlinear, which makes their representation in numerical models an important challenge. Given the already substantial changes observed in the present climate and the limited level of compliance among nations with the international agreements on climate-related emissions, research on climate projections must cover periods beyond the twenty-first century, which implies revisiting and expanding the definition of RCPs.

Another aspect to keep in mind refers to climate change impacts. The effects of a modified climate on many aspects of life (health, freshwater availability,

mobility, food, etc.) or on the environment (effect on plants, transportation, energy generation, fishing, coast-line retreat, etc.) being one of the important lines of research, with even increasingly greater attention in the coming years. A new generation of impact analysis models should be developed to model physical, biological, and economic systems under the effects of climate change. The aim is to provide support to decision makers when targeting for solutions to mitigate and adapt to the effects that, inevitably, are occurring and will occur even with the more optimistic measures to reduce the rate of growth of greenhouse gases concentration in the atmosphere.

Acknowledgments

This work has been partially sponsored by the MINECO of Spain and Feder Funds with the grants CGL2014-52199-R and CGL2017-82868-R.

Further Reading

- Easterling, D.R., Evans, J.L., Groisman, P.Y. et al. (2000). *Bull. Am. Meteorol. Soc.* 81: 417–425.
- Goosse, H. (2015). *Climate System Dynamics and Modelling*. Cambridge University Press.
- Kitchen, D.E. (2013). *Global Climate Change: Turning Knowledge Into Action*. Pearson.
- Meehl, G.A., Zwiers, F., Evans, J. et al. (2000). *Bull. Am. Meteorol. Soc.* 81: 427–436.
- Mooney, C. (2007). *Storm World: Hurricanes, Politics, and the Battle Over Global Warming*. Houghton Mifflin Harcourt.
- Stocker, T.F., Qin, D., Plattner, G.-K. et al. (ed.) (2013). *IPCC, 2013: Climate Change 2013: The Physical Science*

Basis. Contribution of Working Group I to the Fifth Assessment Report of the Intergovernmental Panel on Climate Change, 1535 pp. Cambridge, UK/New York, NY: Cambridge University Press.

- Wolfson, R. (2017). *Energy, Environment and Climate*. W. W. Norton.
- World Meteorological Organization (2013). *The Global Climate 2001–2010: A Decade of Climate Extremes - Summary Report*. Available online: http://library.wmo.int/pmb_ged/wmo_1119_en.pdf (accessed 10 May 2018).

References

- 1 Stocker, T.F., Qin, D., Plattner, G.-K. et al. (ed.) (2013). *IPCC, 2013: Climate Change 2013: The Physical Science Basis. Contribution of Working Group I to the Fifth Assessment Report of the Intergovernmental Panel on Climate Change*, 1535 pp. Cambridge, UK/New York, NY: Cambridge University Press. Available at <http://www.ipcc.ch/report/ar5/wg1/>.
- 2 NASA Global Climate Change (2018). <https://climate.nasa.gov/vital-signs/carbon-dioxide/> (accessed 25 May 2018).
- 3 NASA Global Climate Change (2018). <https://climate.nasa.gov/evidence> (accessed 25 May 2018).
- 4 NOAA Climate.gov (2018). Science & information for a climate-smart nation. <https://www.climate.gov/> (accessed 10 May 2018).
- 5 Met Office Hadley Centre Observations Datasets (2018). <https://www.metoffice.gov.uk/hadobs/hadex2> (accessed 12 May 2018).
- 6 Kovats, R.S. and Ebi, K.E. (2006). *Eur. J. Public Health* 16 (6): 592–599.
- 7 Robine, J.M., Cheung, S.L.K., Le Roy, S. et al. (2008). *C. R. Biol.* 331: 171–178.
- 8 Credit: NASA/Goddard/Earth Observatory (2010). Modis NASA Terra image. https://www.nasa.gov/images/content/485328main_fig1russiaheatwave-full.jpg (accessed 13 November 2018).
- 9 Wikipedia (2018). https://en.wikipedia.org/wiki/2010_Northern_Hemisphere_summerheat_waves (accessed 10 May 2018).
- 10 EM-DAT International Disaster Database (2018). <https://www.emdat.be> (accessed 8 May 2018).
- 11 Amengual, A., Homar, V., Romero, R. et al. (2014). *Int. J. Climatol.* 34: 3481–3498.
- 12 Seneviratne, S.I., Nicholls, N., Easterling, D. et al. (2012). In: *Managing the Risks of Extreme Events and Disasters to Advance Climate Change Adaptation*. (ed. C.B. Field, V. Barros, T.F. Stocker et al.), 109–230. A Special Report of Working Groups I and II of the Intergovernmental Panel on Climate Change (IPCC). Cambridge, UK/New York, NY: Cambridge University Press. Available from http://www.ipcc.ch/pdf/special-reports/srex/SREX-Chap3_FINAL.pdf
- 13 Solomon, S., Qin, D., Manning, M. et al. (ed.) (2007). *IPCC, 2007: Climate Change 2007: The Physical Science Basis. Contribution of Working Group I to the Fourth Assessment Report of the Intergovernmental Panel on Climate Change*, 996 pp. Cambridge, UK/New York, NY: Cambridge University Press.
- 14 Giorgi, F. and Mearns, L.O. (1999). *J. Geophys. Res.: Atmos.* 104 (D6): 6335–6352.
- 15 Giorgi, F. and Lionello, P. (2008). *Glob. Planet. Change* 63 (2–3): 90–104.
- 16 Ramis, C. and Amengual, A. (2018). In: *The Encyclopedia of the Anthropocene*, vol. 2 (ed. D.A. DellaSala and M.I. Goldstein), 209–216. Oxford: Elsevier.
- 17 Jacob, D., Petersen, J., Eggert, B. et al. (2014). *Reg. Environ. Change* 14 (2): 563–578.
- 18 Moss, R., Babiker, W., Brinkman, S. et al. (2008). *Towards New Scenarios for the Analysis of Emissions: Climate Change, Impacts and Response Strategies*, 132 pp. Geneva, Switzerland: Intergovernmental Panel on Climate Change (IPCC).
- 19 Amengual, A., Homar, V., Romero, R. et al. (2012). *J. Clim.* 25: 939–957.
- 20 Cardell, M.F., Romero, R., Amengual, A. et al. (2018). *Int. J. Climatol.* (submitted).
- 21 Haylock, M., Hofstra, N., Klein Tank, A. et al. (2008). *J. Geophys. Res.: Atmos.* 113: D20.
- 22 Cardell, M.F., Amengual, A., Romero, R., and Ramis, C. (2018). *Int. J. Climatol.* (submitted).